nature medicine

Effective and selective targeting of leukemia cells using a TORC1/2 kinase inhibitor

Matthew R Janes[1], Jose J Limon[1], Lomon So[1], Jing Chen[1], Raymond J Lim[1], Melissa A Chavez[1], Collin Vu[2], Michael B Lilly[2], Sharmila Mallya[2], S Tiong Ong[3], Marina Konopleva[4], Michael B Martin[5], Pingda Ren[5], Yi Liu[5], Christian Rommel[5] & David A Fruman[1]

Targeting the mammalian target of rapamycin (mTOR) protein is a promising strategy for cancer therapy. The mTOR kinase functions in two complexes, TORC1 (target of rapamycin complex-1) and TORC2 (target of rapamycin complex-2); however, neither of these complexes is fully inhibited by the allosteric inhibitor rapamycin or its analogs. We compared rapamycin with PP242, an inhibitor of the active site of mTOR in both TORC1 and TORC2 (hereafter referred to as TORC1/2), in models of acute leukemia harboring the Philadelphia chromosome (Ph) translocation. We demonstrate that PP242, but not rapamycin, causes death of mouse and human leukemia cells. *In vivo*, PP242 delays leukemia onset and augments the effects of the current front-line tyrosine kinase inhibitors more effectively than does rapamycin. Unexpectedly, PP242 has much weaker effects than rapamycin on the proliferation and function of normal lymphocytes. PI-103, a less selective TORC1/2 inhibitor that also targets phosphoinositide 3-kinase (PI3K), is more immunosuppressive than PP242. These findings establish that Ph$^+$ transformed cells are more sensitive than normal lymphocytes to selective TORC1/2 inhibitors and support the development of such inhibitors for leukemia therapy.

The PI3K-AKT-mTOR signaling axis is central to the transformed phenotype of most cancer cells[1]. PI3K is a lipid kinase whose products mediate membrane assembly of signaling complexes downstream of activated tyrosine kinases and the small GTPase Ras. AKT serine-threonine kinases are activated in a PI3K-dependent manner to phosphorylate numerous substrates, thereby promoting cell growth, proliferation and survival[2]. Most tumor cells bear mutations that increase PI3K-AKT-mTOR signaling output[1,3], and activation of this pathway has been linked to chemoresistance in a variety of clinical settings[4,5]. Therefore, priority has been given to the development of anticancer agents targeting PI3K, AKT or downstream enzymes such as mTOR[6]. However, this signaling network mediates essential physiological functions and is subject to complex cross-talk and feedback, which has complicated efforts to identify an optimal pharmacological profile to achieve effective and selective killing of cancer cells.

The mTOR kinase is present in two cellular protein complexes, TORC1 and TORC2, which have distinct subunit composition, substrates and mechanisms of activation (**Fig. 1a**)[7,8]. The best-known substrates of TORC1 are S6 kinase (S6K) and 4E-BP1 (eukaryotic initiation factor 4E-binding protein-1); the main substrates of TORC2 are AKT and related kinases. Rapamycin (sirolimus) and its analogs, such as RAD001 (everolimus) and CCI-779 (temsirolimus), suppress mTOR activity through an allosteric mechanism that acts at a distance from the ATP-catalytic binding site[6,9,10]. Members of this class of mTOR inhibitor have profound immunomodulatory activity[11,12] but have achieved limited success as anticancer agents[9]. Mechanistically, rapamycin has two main drawbacks (**Fig. 1a**). First, the drug suppresses TORC1-mediated S6K activation, thereby blocking a negative feedback loop, but does not acutely inhibit TORC2. In many cancer cells, this leads to elevated PI3K-AKT signaling and promotes cell survival[10]. Second, rapamycin is an incomplete inhibitor of TORC1, reducing phosphorylation of 4E-BP1 only partially in most cell contexts[13–17].

A promising approach to overcome these limitations is through ATP-competitive 'active-site' mTOR inhibitors. One strategy has been to use small-molecule TORC1/2 inhibitors that also inhibit PI3K lipid kinases (**Fig. 1a**)[6]. One such compound, PI-103, is more potent than rapamycin in mouse models of leukemia and in primary human leukemia colony assays[18–21]. However, the clinical therapeutic efficacy and tolerability of such dual PI3K-mTOR inhibitors remain to be established. Recently, four independent groups reported the discovery and characterization of selective ATP-competitive TORC1/2 inhibitors[14–17]. Active-site mTOR inhibitors strongly suppress 4E-BP1 phosphorylation and reduce phosphorylation of TORC2 substrates, including AKT (**Fig. 1a**), without strongly inhibiting PI3K[14–17]. Here we report a comparison of the effects of rapamycin and a selective TORC1/2 inhibitor, PP242, in models of leukemia and on normal lymphocyte function. We demonstrate that PP242 has potent cytotoxic activity against leukemia cells and enhances the efficacy of the tyrosine kinase inhibitors (TKIs) imatinib and dasatinib in Ph$^+$ acute leukemia models. The effects of PP242 are similar to those of pan–PI3K-TORC1/2 inhibitors but stronger than those of

[1]Institute for Immunology and Department of Molecular Biology & Biochemistry and [2]Division of Hematology/Oncology, Department of Medicine, University of California–Irvine, Irvine, California, USA. [3]Duke-National University of Singapore Graduate Medical School, Singapore. [4]Section of Molecular Hematology and Therapy, Departments of Stem Cell Transplantation and Cellular Therapy, University of Texas, M.D. Anderson Cancer Center, Houston, Texas, USA. [5]Intellikine Inc., La Jolla, California, USA. Correspondence should be addressed to D.A.F. (dfruman@uci.edu).

Received 2 November 2009; accepted 23 December 2009; published online 13 January 2010; doi:10.1038/nm.2091

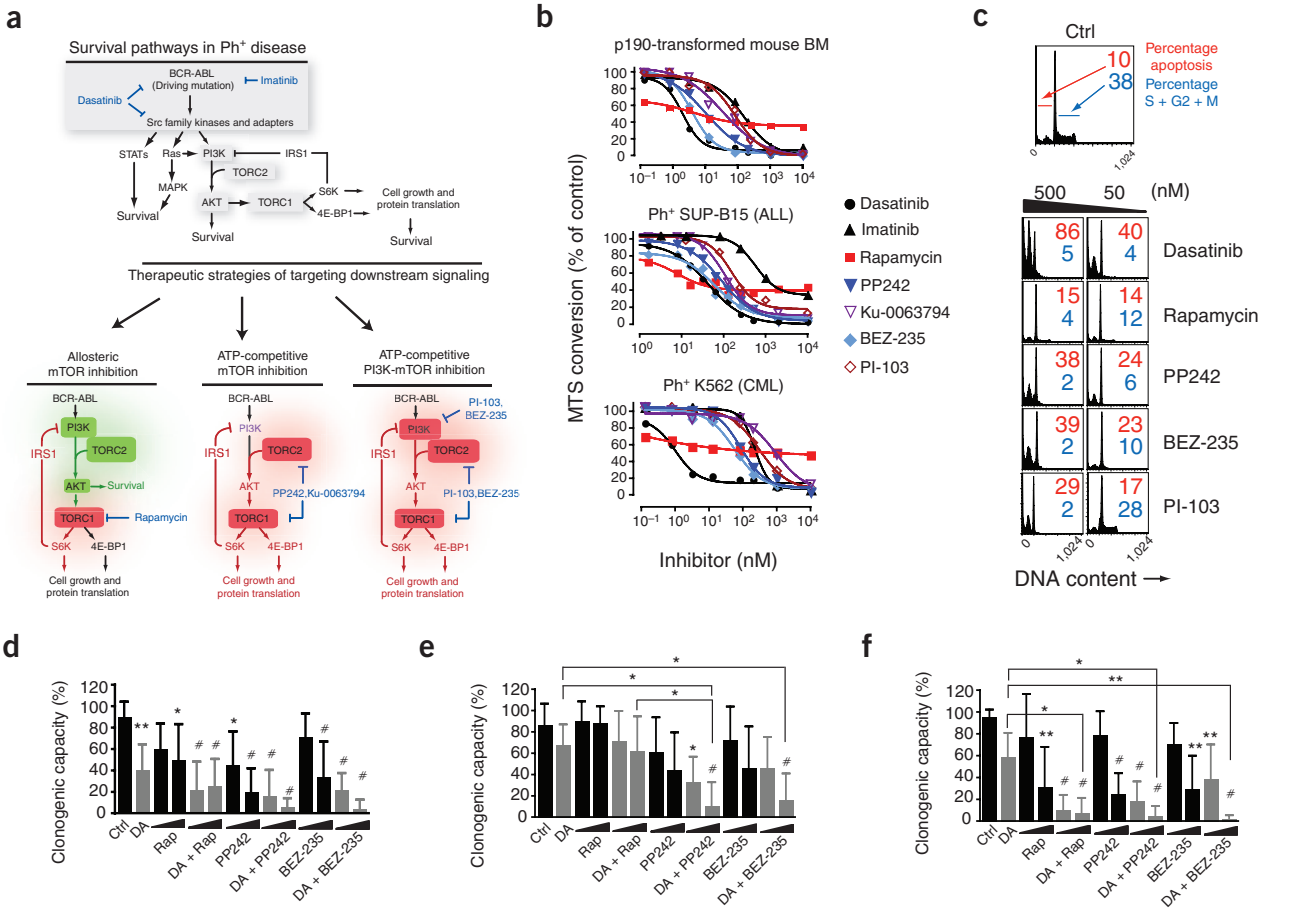

Figure 1 PP242 induces apoptosis of p190 BCR-ABL–transformed mouse hematopoietic progenitors and human Ph+ B-ALL cells *in vitro*. (**a**) Schematic model of BCR-ABL–driven mechanisms of leukemia cell survival (top). Models of incomplete mTOR inhibition (bottom left) versus complete and selective mTOR inhibition (bottom middle) versus both PI3K and mTOR inhibition (bottom right) in Ph+ disease. Green, activated; red, inhibited. Selective mTOR inhibitors (middle) may affect PI3K (purple) differently depending on the degree of off-target inhibition of PI3K. STAT, signal transducer and activator of transcription; MAPK, mitogen-activated protein kinase; IRS1, insulin receptor substrate 1. (**b**) The number of viable mouse p190, human SUP-B15 or human K562 cells after 48 h of treatment with the indicated inhibitors, as determined by the MTS conversion assay ($n = 3$–9 independent experiments, error bars omitted for clarity). BM, bone marrow. (**c**) DNA content, as measured by flow cytometry, in p190 cells cultured for 24 h with the indicated inhibitors. Representative of three independent experiments. (**d**–**f**) Anticlonogenic effects of TORC1/2 and pan-PI3K-TORC1/2 inhibitors with and without dasatinib in primary Ph+ leukemias. Purified bone marrow or peripheral blood from untreated, newly diagnosed individuals with Ph+ B-ALL ($n = 8$) (**d**), relapsed or refractory Ph+ B-ALL ($n = 6$) (**e**) or imatinib-resistant blast crisis (BC)-CML ($n = 4$ for lymphoid BC-CML and $n = 1$ for myeloid BC-CML) (**f**) were assessed for colony formation potential in MethoCult cultures with dasatinib (DA; 5 nM) alone or in combination with increasing concentrations (20 or 200 nM) of rapamycin (Rap), PP242 or BEZ-235. Colony numbers were normalized to the vehicle control for each human specimen and reported as the mean ± s.d., with n = total number of individual specimens as listed above, each tested once (*$P < 0.05$, **$P < 0.01$, #$P < 0.001$, repeated-measures analysis of variance (ANOVA), measured versus the vehicle control (Ctrl), except where indicated by brackets). **Supplementary Table 4** contains a more detailed description of the human leukemic samples.

rapamycin. We also report an unexpected reversal of potency, such that rapamycin produces much stronger immunosuppression than PP242 in a set of *in vitro* and *in vivo* assays of adaptive immune function. At doses that show therapeutic effects in leukemia models, the pan–PI3K-TORC1/2 inhibitor PI-103 is also more immunosuppressive than PP242. Thus, selective TORC1/2 inhibitors might achieve a favorable balance of efficacy and tolerability that is superior to other approaches targeting this pathway in cancer.

RESULTS

Selective TORC1/2 inhibition causes death of BCR-ABL+ cells

The structure and selectivity of the pyrazolopyrimidine compound PP242 have been reported previously[14], and further drug-related information is provided in **Supplementary Table 1**. We tested the efficacy of PP242 in models of Ph+ B precursor acute lymphoblastic leukemia (B-ALL), a subtype of leukemia initiated by the *BCR-ABL* oncogene that arises from the Philadelphia chromosome translocation[22,23]. When mouse bone marrow cells are infected with a retrovirus expressing human p190 BCR-ABL (p190 is the isoform of BCR-ABL most commonly detected in Ph+ B-ALL), transformed progenitor B cell lines (termed p190 cells) emerge that initiate aggressive B-ALL upon transfer to recipient mice[19,24]. We monitored the proliferation and survival of p190 cells treated with mTOR inhibitors in comparison to the TKIs imatinib and dasatinib that are currently used in the clinic to suppress BCR-ABL tyrosine kinase activity (**Fig. 1b** and **Supplementary Table 2**). Using a colorimetric assay (MTS (3-(4,5-dimethylthiazol-2-yl)-5-(3-carboxymethoxyphenyl)-2-(4-sulfophenyl)-2H-tetrazolium) conversion), we observed that both imatinib and dasatinib fully suppressed cell growth, as expected (**Fig. 1b** and **Supplementary Table 2**). Rapamycin had antiproliferative effects (50% growth

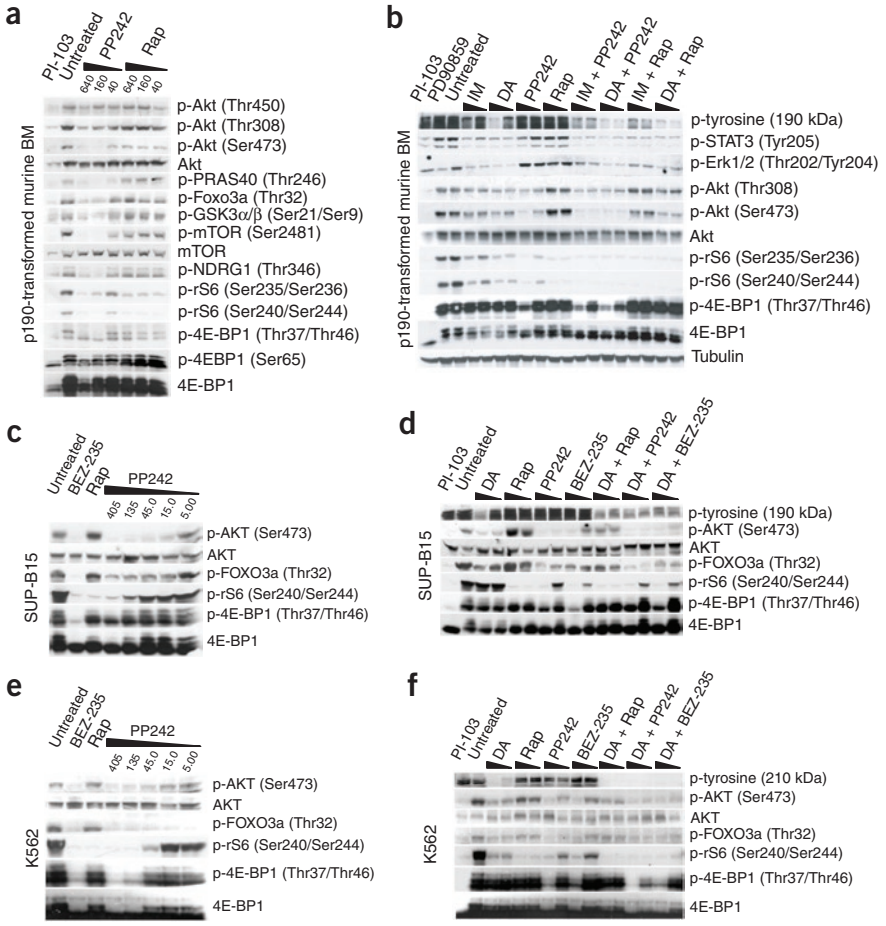

Figure 2 PP242 completely inhibits TORC1 and TORC2 signaling in BCR-ABL$^+$ cells, whereas rapamycin partially suppresses TORC1 and drives elevated PI3K-AKT signaling. (**a**,**b**) Western blots of lysates from p190 cells treated for 1.5 h (**a**) or 3 h (**b**) with the indicated inhibitors. Cells were treated with imatinib (IM; 0.5 and 1.0 μM), DA (5 and 50 nM), PP242 and rapamycin (Rap) (50 and 400 nM). IM (1.0 μM) and DA (100 nM) were used for the combination treatments. PD98059 is an inhibitor of Mek (mitogen-activated protein kinase kinase). Slashes indicate that the antibodies used recognize the indicated forms of the protein. (**c**–**f**) Western blots of lysates from SUP-B15 (**c**,**d**) or K562 (**e**,**f**) cells treated for 3 h with the indicated inhibitors. The numbers shown in panels **a**, **c** and **e** denote inhibitor concentrations in nM. (**a**–**f**) Representative of two to five experiments.

inhibitory concentration (GI_{50}) = 6.5 nM), but reached a plateau in efficacy at ~60% inhibition of cell growth. In contrast, PP242 suppressed cell growth by >90%, with low nanomolar potency (GI_{50} = 12 nM). The selective TORC1/2 inhibitor Ku-0063794 (ref. 15), which is structurally unrelated to PP242, also fully suppressed growth, although with lesser potency (GI_{50} = 36 nM). We also tested two agents that inhibit both class I PI3Ks and TORC1/2 through an ATP-competitive mechanism, PI-103 (ref. 25) and BEZ-235 (ref. 26). As we previously reported[19], pan–PI3K-TORC1/2 inhibition fully suppressed growth of p190 cells (GI_{50} = 86 nM for PI-103, GI_{50} = 4 nM for BEZ-235). We obtained similar relative GI_{50} values when we compared the effects of these compounds on the human Ph$^+$ B-ALL cell line SUP-B15 and the Ph$^+$ chronic myeloid leukemia (CML) cell line K562 (**Fig. 1b** and **Supplementary Table 2**). Cell cycle analysis confirmed that TORC1/2 inhibitors and pan–PI3K-TORC1/2 inhibitors caused both cell cycle arrest and death, whereas rapamycin was primarily cytostatic (**Fig. 1c**).

We also observed a greater antiproliferative potency of PP242 relative to rapamycin in a panel of solid tumor cell lines carrying either PI3K gain of function or PTEN (phosphatase and tensin homolog) loss of function mutations (**Supplementary Table 3**), indicating a generally stronger anticancer effect of TORC1/2 inhibitors; this is in agreement with a recently reported study of TORC1/2 inhibitors in solid tumor lines[17]. The GI_{50} of PI-103 was consistently at least two times higher than that of PP242 in these assays (**Supplementary Tables 2a** and **3**).

PP242 enhances the antileukemic effects of TKIs *in vitro*

Imatinib provides poor long-term survival in Ph$^+$ B-ALL[27,28]. Relapse of both Ph$^+$ B-ALL and blast crisis CML are often due to mutations in the BCR-ABL kinase domain that cause resistance to imatinib. Second-generation ABL TKIs such as dasatinib suppress the activity of some imatinib-resistant BCR-ABL variants (for example, those with Y253H or E255K mutations) but not others (those with T315I mutations). Targeting signaling pathways downstream of BCR-ABL, such as with TORC1/2 inhibition, might overcome this resistance[29,30]. Our observation that PP242 causes apoptosis (**Fig. 1c**) further suggested that TORC1/2 inhibitors might overcome resistance to TKIs and also synergize with TKIs to kill leukemia cells. Indeed, transformation of mouse bone marrow cells with BCR-ABL was inhibited to a similar extent by PP242 when comparing its effects on wild-type p190 BCR-ABL or mutants (Y253H, E255K or T315I) (**Supplementary Fig. 1a**). Furthermore, PP242 strongly synergized with imatinib in suppressing the growth of cells expressing wild-type p190, similar to the potency achieved with BEZ235 and imatinib (**Supplementary Fig. 1b** and **Supplementary Table 2**). This synergistic effect of PP242 with imatinib was superior to that of rapamycin with imatinib (**Supplementary Fig. 1b** and **Supplementary Table 2**).

We further tested the effects of PP242 alone or when combined with ABL inhibitors on primary human Ph$^+$ B-ALL cells, including samples from newly diagnosed cases and from drug-resistant relapses (**Fig. 1d**,**e** and **Supplementary Table 4** for subject characteristics). For these experiments, we used dasatinib to inhibit BCR-ABL, as this agent is emerging as a favored TKI for Ph$^+$ B-ALL treatment, either as a monotherapy or combined with chemotherapy[27,31]. PP242 significantly reduced colony formation in samples of newly-diagnosed Ph$^+$ B-ALL and augmented the effect of dasatinib in samples derived from subjects who had relapsed after combination chemotherapy with imatinib (**Fig. 1d**,**e**). BEZ235 had a similar potency to PP242 when tested alone or with dasatinib, whereas rapamycin had a lesser effect in these sample groups and did not augment dasatinib efficacy (**Fig. 1d**,**e**). In five samples obtained from cases of blast crisis-stage Ph$^+$ CML, rapamycin was equally effective as PP242 or BEZ-235 (**Fig. 1f**).

PP242 and rapamycin have distinct effects on TORC1/2 outputs

In fibroblasts and solid tumor cell lines, active-site mTOR inhibitors suppress rapamycin-resistant outputs of TORC1 and TORC2 (refs. 14–17). Similarly, in p190 cells, PP242 suppressed phosphorylation

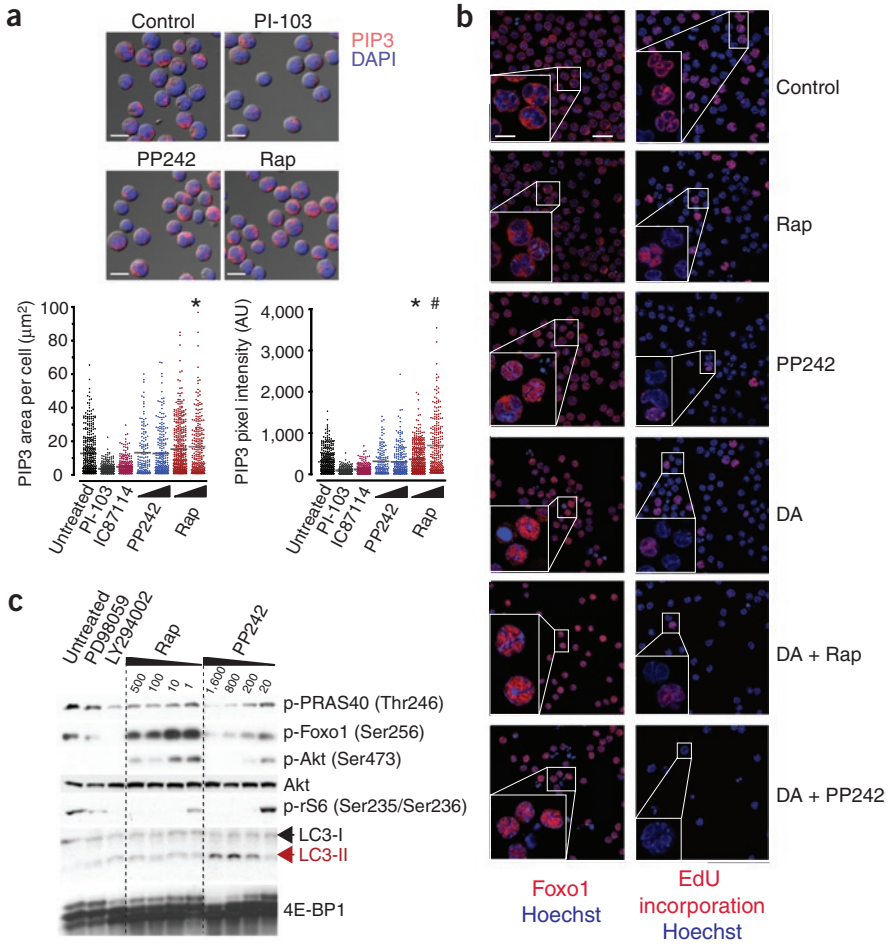

Figure 3 Immunofluorescence analysis shows that PP242 induces Foxo1 nuclear entry without affecting PIP3 abundance. (**a**) Activation of PI3K, as quantified in cells by measuring the localized area of PIP3 accumulation and the PIP3 signal pixel intensity by confocal microscopy (*$P < 0.05$, #$P < 0.001$, ANOVA, measured versus the control). p190 cells were cultured for 4 h with PI-103 (2 μM), the PI3K inhibitor IC87114 (10 μM), PP242 (20 and 200 nM) or rapamycin (Rap) (20 and 200 nM). A minimum of 250 cells was quantified from two separate images. Representative images depict PIP3 accumulation, nuclear content (DAPI stain) merged onto differential interference contrast images. Scale bar, 13.5 μm. AU, arbitrary units. (**b**) p190 cells were cultured for 8 h in chamber wells with DA (10 nM), PP242 (250 nM), BEZ-235 (250 nM) or Rap (250 nM) and pulsed with 5-ethynyl-2-deoxyuridine (EdU) 1 h before fixation. Cell proliferation (EdU accumulation) and localization of Foxo1 were assessed by confocal microscopy (scale bar, 22.5 μm), and representative cells were magnified for clarity (scale bar, 10 μm). Hoechst is a nuclear stain. (**c**) Western blot analysis of lysates from p190 cells treated with the Mek inhibitor PD98059 (10,000 nM), LY294002 (1,000 nM) and the indicated concentrations (in nM) of Rap and PP242 for 24 h. Results in **b** and **c** are representative of two independent experiments.

of the Ser473 residue of Akt, a TORC2 phosphorylation site, whereas rapamycin treatment caused an increase over time in Ser473 phosphorylation as well as in phosphorylation of the PDK1 (phosphoinositide-dependent kinase-1) site Thr308 (**Fig. 2a**,**b**). Although both drugs effectively suppressed phosphorylation of the ribosomal S6 protein (rS6), only PP242 decreased phosphorylation of 4E-BP1 (**Fig. 2a**,**b**). These distinct phosphoprotein signatures of PP242 and rapamycin remained apparent when the drugs were combined with clinically achievable concentrations of ABL kinase inhibitors (**Fig. 2b**); p4E-BP1 and pAkt amounts were more effectively suppressed by treatment with TKIs plus PP242 as compared to treatment with TKIs plus rapamycin. Notably, TKIs alone did not fully suppress TORC1/2 signaling (**Fig. 2b**), as has been observed previously in other BCR-ABL–driven cell models[32,33]. We obtained similar results with SUP-B15 and K562 cells (**Fig. 2c–f**). Cap-dependent messenger RNA translation is facilitated by TORC1-mediated phosphorylation of 4E-BP1, which releases this inhibitory protein from eukaryotic initiation factor 4E (eIF4E) (refs. 7,8). PP242 treatment of p190 cells increased binding of 4E-BP1 to eIF4G with a concomitant decrease in binding of 4E-BP1 to eIF4E, whereas rapamycin had little effect (**Supplementary Fig. 2**).

Although PP242 at high concentrations can inhibit PI3K enzymes *in vitro*[14], the drug did not alter cellular production of the PI3K product phosphatidylinositol-3,4,5-trisphosphate (PIP_3) in p190 cells (**Fig. 3a**). In contrast, rapamycin treatment increased PIP_3 production (**Fig. 3a**). It is possible that PP242 counteracts feedback activation of PI3K through its ability to weakly inhibit PI3K enzymes at concentrations that fully inhibit TORC1/2.

To assess TORC2 function, we examined the phosphorylation and localization of forkhead box O (Foxo) transcription factors, which are substrates of both Akt and serum- and glucocorticoid-induced kinase downstream of TORC2 (refs. 34,35). PP242, but not rapamycin, reduced Foxo phosphorylation on Akt consensus sites (**Fig. 2a**,**c–f**) and caused nuclear accumulation of Foxo1 in p190 cells correlating with greater inhibition of cell cycling (**Fig. 3b**). PP242, but not rapamycin, also decreased mTOR autophosphorylation on Ser2481, phosphorylation of the Akt substrates glycogen synthase kinase-3 (GSK3) and proline-rich Akt substrate of 40 kDa (PRAS40) and phosphorylation of the serum- and glucocorticoid-induced kinase-1 substrate N-myc downstream regulated gene-1 (NDRG1), all indicators of TORC2 activity[14–17,36,37] (**Fig. 2a**). Thus, PP242 blocked all TORC1 and TORC2 outputs tested without altering PIP_3 levels. PP242 also seemed to increase autophagy more than did rapamycin in p190 cells, as indicated by accumulation of LC3-II (**Fig. 3c**).

PP242 suppresses leukemia better than rapamycin *in vivo*

To compare the pharmacological characteristics and antileukemic efficacy of mTOR inhibitors alone or in combination with TKIs *in vivo*, we used three models: a mouse model of $p190^{BCR\text{-}ABL}$ pre-B lymphoid leukemia transplanted into syngeneic recipients; a bioluminescent xenograft model of human SUP-B15 cells stably expressing luciferase and transplanted into immunocompromised nonobese diabetic, severe combined immunodeficient, interleukin-2 receptor-γ–knockout mice (NSG mice[38]); and a xenograft model in which four independent leukemia specimens were transplanted into NSG mice.

The mouse p190 model produces reproducible engraftment and fatal leukemia in recipients that are either irradiated or nonirradiated; the disease in these mice has pathologic features resembling those of human B-ALL[24]. This model is convenient for both survival measurements and pharmacodynamic monitoring. In this model,

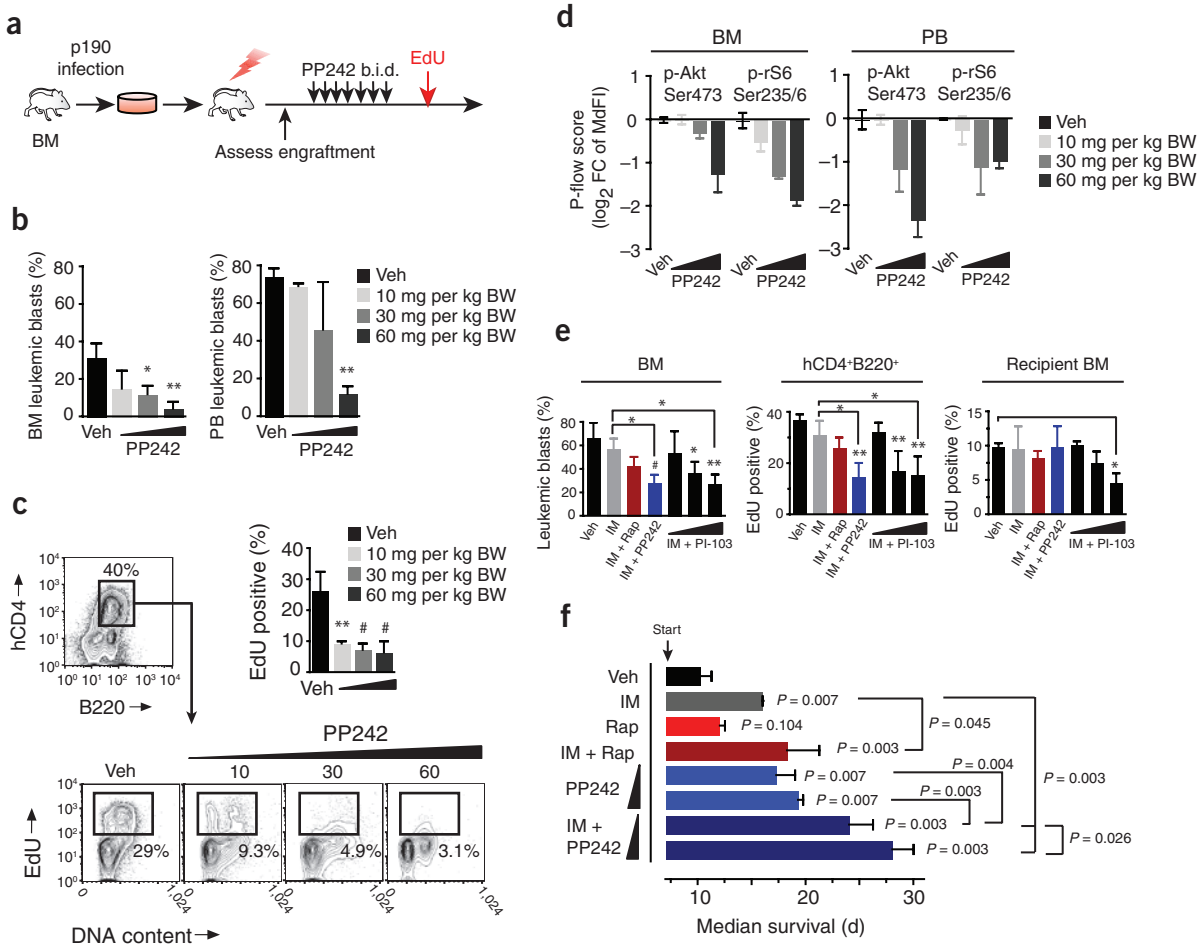

Figure 4 PP242 selectively suppresses leukemic expansion *in vivo* and extends survival. (**a**–**d**) Short-term antileukemic efficacy of PP242 in conditioned recipients (450 rad) engrafted with mouse p190 cells ($n = 3$ per treatment group). (**a**) Schematic of treatment design in which mice injected intravenously with p190 cells were treated (by oral gavage, also termed per oral and hereafter abbreviated p.o.) twice daily (b.i.d.) starting on day 7 after transplant for 4 d with PP242 or vehicle (Veh, PEG400). (**b**) Leukemic burden in bone marrow and peripheral blood (PB) (mean percentage ± s.d., ANOVA, measured versus vehicle-treated mice), as assessed by flow cytometry. BW, body weight. (**c**) The percentage of leukemic cells actively cycling (EdU^+) was measured by flow cytometry (mean ± s.d., ANOVA, measured versus vehicle-treated mice). (**d**) Pharmacodynamic analysis of PP242. Flow cytometry was used to quantify intracellular levels of p-Akt (Ser473) and p-rS6 (Ser235 and Ser236) in leukemic cells (expressing the human CD4 (hCD4) marker and the B cell surface protein B220) from the bone marrow and peripheral blood of recipient mice. P-flow scores were obtained by $\log_2$ transformation of the fold change (FC) of the median fluorescent intensity (MdFI) of p-Akt or p-rS6 and then graphed as the mean ± s.d. FC was calculated from the averaged MdFI of PP242 treated samples ($n = 3$ per group) divided by the averaged MdFI of vehicle treated samples ($n = 3$). (**e**) Short-term treatment study comparing p190 leukemia burden as in **a**, but using nonirradiated mice and comparing combinations of IM (150 mg per kg body weight intraperitoneally (i.p.) daily) with Rap (7 mg per kg body weight i.p daily), PP242 (60 mg per kg body weight p.o. daily) or various doses of PI-103 (10, 30 or 60 mg per kg body weight i.p., b.i.d.). Graphs show leukemic burden in the bone marrow (left) or the percentage cycling cells among leukemic $hCD4^+$ cells (middle) or host $hCD4^-$ bone marrow cells (right), $n = 4$ per group for vehicle- and IM-treated mice, and $n = 3$ for other remaining treatment groups (mean ± s.d.). (**f**) Mice injected with p190 cells were treated daily starting on day 7 after transplantation with IM (150 mg per kg body weight, i.p.), Rap (7 mg per kg body weight, i.p.) or PP242 (30 and 60 mg per kg body weight, p.o.). Mice were followed daily for survival ($n = 5$ per group, median ± interquartile range, measured versus vehicle-treated mice, except where indicated by brackets). 'Start' indicates the start of drug treatment.

short-term oral dosing with PP242 significantly reduced leukemic burden in the spleen and bone marrow in a dose-dependent manner, which correlated with inhibition of cell cycle progression and induction of apoptosis in the leukemia cells (**Fig. 4a–d** and **Supplementary Figs. 3–5**). These effects were associated with inhibition of TORC1 and TORC2 substrate phosphorylation and a smaller leukemic cell size (**Fig. 4d** and **Supplementary Fig. 3**). PI-103 (60 mg per kg body weight twice per day (b.i.d.)) treatment significantly potentiated the effects of imatinib in this model (**Fig. 4e**), similarly to our previous findings[19]. In contrast, mice treated with rapamycin showed no significant reduction in leukemic burden (**Fig. 4e** and **Supplementary Fig. 4**). This was not due to poor bioavailability, because rapamycin treatment caused strong inhibition of rS6 phosphorylation (**Supplementary Fig. 4**) and was severely immunosuppressive at this dose, as discussed below. We also detected decreased phosphorylation of Akt on Ser473 in rapamycin-treated mice, consistent with reports that rapamycin can inhibit assembly of TORC2 after extended exposure to the drug[39].

In a long-term survival study, oral dosing of PP242 (30 and 60 mg per kg body weight) significantly delayed the onset of leukemia (**Fig. 4f**). Rapamycin had no effect on its own in this setting but augmented the protective effect of a suboptimal dose of imatinib (150 mg per kg body

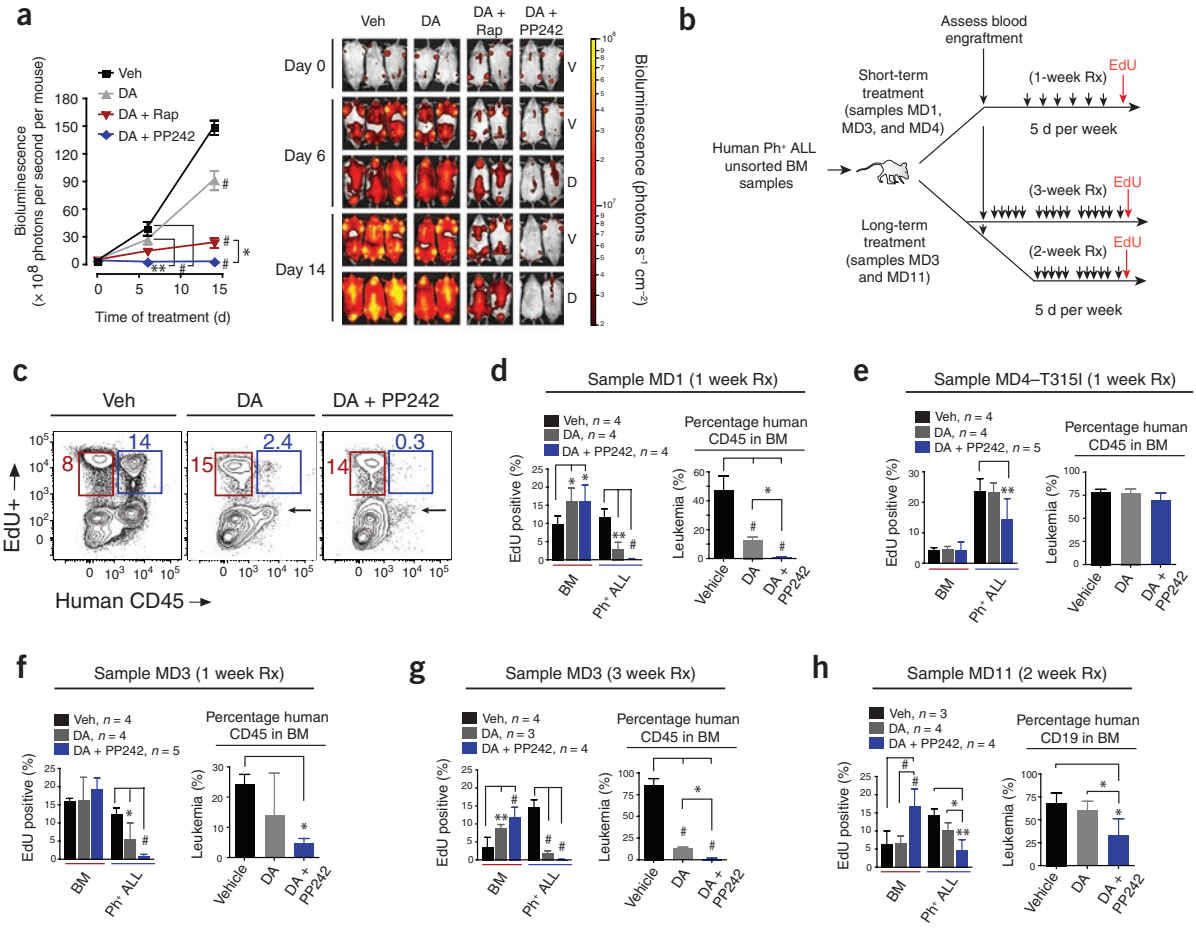

Figure 5 PP242 enhances the efficacy of dasatinib and the combination causes regression of human Ph+ B-ALL xenografts. (**a**) Sequential bioluminescent imaging of leukemia development after SUP-B15^{ffLuc} cells were injected into NSG mice. The scale on the right shows the color scheme for low (red) to high (yellow) photon flux. Both ventral (V) and dorsal (D) images were taken, allowing detection of luminescent cells in the brain and spinal cord. Representative images are shown. The graph on the left shows the bioluminescence (photon flux) detected in each treatment group (mean ± s.d., repeated measures ANOVA): vehicle ($n = 4$), DA (2.5 mg per kg body weight, $n = 5$) or DA combined with PP242 (60 mg per kg body weight, $n = 5$) or combined with Rap (7.5 mg per kg body weight, $n = 5$). *$P < 0.05$, ** $P < 0.01$, #$P < 0.001$, ANOVA, measured versus the control, except where indicated by brackets. (**b**) Schematic of treatment design for xenografts of primary human Ph+ B-ALL samples. Cohorts of mice transplanted with human specimens were assessed for engraftment 35–90 d after transplant (MD4, 35 d; MD1, 40 d; MD3, 40 or 44 d; and MD11, 90 d) and randomized into the indicated treatment groups. Cohorts of NSG mice with similar human engraftment were treated daily by oral gavage for 5 consecutive d per week (samples MD1, MD3 and MD4 for 1 week, MD11 for 2 weeks and MD3 for 3 weeks) with DA (5 mg per kg body weight), DA combined with PP242 (60 mg per kg body weight) or vehicle. Cohorts of engrafted NSG mice that completed the indicated treatment schedule were injected with EdU (i.p.) 1 h after the last treatment dose to assess proliferative capacity. After 1 h of EdU distribution, all mice per treatment groups per cohort were killed. (**c–h**) Quantification of leukemic burden (mean ± s.d., ANOVA) and the percentage of cycling cells (mean ± s.d., two-way ANOVA) in the bone marrow was assessed by flow cytometry. (**c**) Cell cycling was measured by EdU incorporation into cells (EdU+), with the numbers indicating the percentages of cycling cells within the normal marrow (red gate) and leukemic (blue gate) cell populations. A representative bone marrow sample from each treatment group of the MD1 cohort is depicted. Arrows signify selective regression of leukemia (human CD45+) cells relative to endogenous bone marrow (human CD45−). The total leukemic burden (**d–h**) was determined from the percentage of hCD45- or hCD19-positive cells in the bone marrow. *$P < 0.05$, **$P < 0.01$, #$P < 0.001$.

weight), as previously reported[40]. The combination of PP242 with imatinib provided the greatest survival benefit, with two of five mice showing minimal disease (2–20% in the bone marrow) one month after initiation of treatment (**Fig. 4f** and **Supplementary Fig. 3b**).

In the xenograft models, we focused on the ability of PP242 to enhance the efficacy of dasatinib, an emerging standard of care for treatment of patients with Ph+ B-ALL. This experimental approach was motivated in part by the greater efficacy of combination treatments in human Ph+ B-ALL colony assays (**Fig. 1**) and also by the likelihood that new active-site mTOR inhibitors will be tested clinically in combination with approved TKIs. The SUP-B15–luciferase xenograft model allowed us to perform quantification of leukemia cell expansion over time using sequential bioluminescent imaging and to correlate these results with signaling differences observed in SUP-B15 cells treated with drug combinations *in vitro* (**Fig. 2c,d**). We chose a daily dose of dasatinib reported to be efficacious in K562 xenografts (2.5 mg per kg body weight)[41]. This dose modestly delayed SUP-B15 expansion *in vivo* (**Fig. 5a**), providing a useful system to test for improved efficacy of combination treatments. Although rapamycin enhanced the effect of dasatinib, leukemic burden continued to increase with this combination (**Fig. 5a**). In contrast, the combination of dasatinib with PP242 caused regression of leukemic disease and prevented dissemination to the central nervous system (**Fig. 5a**).

In xenograft experiments using primary human leukemia samples, we tested PP242 in combination with a higher dose of dasatinib (5 mg

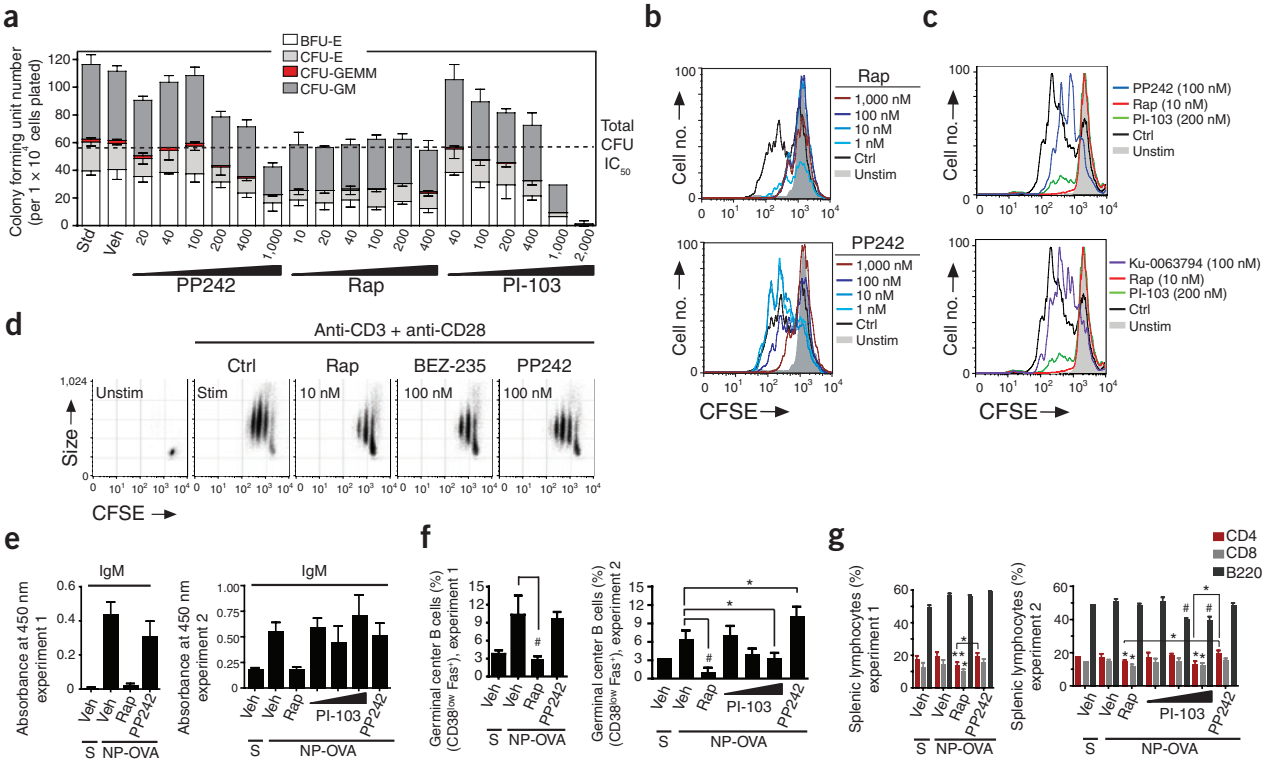

Figure 6 *In vitro* and *in vivo* effects of PP242 compared to rapamycin in assays of normal immune cell proliferation and function. (**a**) Quantification of the number of erythroid and myeloid hematopoietic clonogenic progenitors in bone marrow cells from a healthy human donor, as assessed by colony formation in the presence of the indicated concentrations (in nM) of inhibitors. The anticlonogenic effects of the indicated inhibitors were assessed in triplicate cultures (mean ± s.d.). and the level of 50% inhibition of total colony growth is depicted. BFU-E, blast-forming unit, erythroid; CFU-E, colony-forming unit, erythroid; CFU-GEMM, colony-forming unit, granulocyte, erythrocyte, monocyte, megakaryocyte; CFU-GM, colony-forming unit, granulocyte, macrophage; IC_{50}, 50% inhibitory concentration. (**b**–**d**) Cell division tracking of mouse lymphocytes, as assessed by labeling cells with CFSE before incubation for 3 d with the indicated stimuli. Reduced CFSE fluorescence indicates that cell division has occurred. The histogram overlays (**b**,**c**) show the cell division history of CFSE-labeled B cells pretreated with Rap, PP242, PI-103 or Ku-0063794 15 min before stimulation with IgM-specific antibody (**b**) or lipopolysaccharide (**c**) in the continuing presence of inhibitor. In **b** and **c**, the top and bottom histograms are from the same experiment. Dot plots (**d**) depict CFSE fluorescence versus cell size (forward scatter) of T cells activated with antibody to CD3 and antibody to CD28 or unstimulated (unstim.). Where indicated, cells were pretreated and cultured with Rap, PP242 or BEZ-235 or with vehicle (Ctrl). Representative examples of 3–5 independent experiments are shown. (**e**–**g**) Mice ($n = 3$ or 4 per group) were immunized with NP-OVA in alum (i.p.), and immune responses were measured 8 d later. Mice were treated with vehicle (Veh), Rap (7.5 mg per kg body weight, i.p.,daily), PP242 (60 mg per kg body weight, p.o. daily) or PI-103 (10, 30 or 60 mg per kg body weight, i.p., b.i.d.) starting one day before immunization. S, sham immunized. (**e**) Quantification of nitrophenyl-specific IgM in serum by ELISA (mean ± s.d.); equivalent results were obtained for nitrophenyl-specific IgG1 (data not shown). (**f**,**g**) Quantification of the percentage of splenic germinal center B cells ($CD38^{low}Fas^{+}$, gated on $B220^{+}IgD^{-}$) (**f**), splenic total B cells ($B220^{+}$) and splenic T cell subsets ($CD4^{+}$ and $CD8^{+}$) (**g**) (mean ± s.d.) by flow cytometry. $^{*}P < 0.05$, $^{**}P < 0.01$, $\#P < 0.001$, ANOVA, measured versus vehicle-treated, NP-OVA–immunized mice, except where indicated by brackets. (**e**,**f**) Results are depicted from two independent experiments (experiment 1 and 2) using the same experimental design.

per kg body weight) that significantly suppressed expansion of some Ph^{+} B-ALL samples (MD1 and MD3) but not others (MD4 and MD11) (**Fig. 5b–h** and **Supplementary Fig. 6**; **Supplementary Table 4** contains subject characteristics). The combination of PP242 and dasatinib significantly decreased leukemia burden, leukemia cell cycling or both (**Fig. 5b–h** and **Supplementary Fig. 6**). Dasatinib combined with PP242 was more effective than dasatinib alone in a short-term (1-week) treatment study of sample MD1 and in a long-term (3-week) treatment study of sample MD3 (**Fig. 5c**,**d**,**g**). Dasatinib plus PP242 caused apoptosis of human $CD19^{+}$ cells in the bone marrow of xenograft recipients; concurrently, endogenous hematopoietic cells of the recipient mice showed recovery of cell cycling (**Fig. 5c**,**d**,**g–h** and **Supplementary Fig. 6b**). Sample MD4 (which carried the T315I mutated form of BCR-ABL) showed less proliferation in xenografted mice treated with dasatinib plus PP242 (**Fig. 5e**), and although the leukemic burden in the bone marrow was not significantly affected, the spleen weight was reduced (**Supplementary Fig. 6c**). For sample MD11, which showed dasatinib resistance in the bone marrow despite no detectable *BCR-ABL* mutations, a 2-week treatment with dasatinib plus PP242 lowered leukemic burden, proliferation and spleen weight (**Fig. 5h** and **Supplementary Fig. 6c**). The greater response of MD11 relative to MD4 might have resulted from a difference in leukemic burden at the start of treatment, the different lengths of treatment or leukemia-specific genetic differences. We did not observe drug-related toxicity in mice at therapeutic doses of PP242 (**Supplementary Fig. 6d** and data not shown).

TORC1/2 inhibitors are less immunosuppressive than rapamycin

Rapamycin and its analogs are immunosuppressive and myelosuppressive[42]. In contrast, in mice treated with PP242 we observed a highly selective response of leukemia cells compared to normal hematopoietic cells. PP242 prevented infiltration of the spleen and lymph nodes by p190 cells while largely preserving the normal splenic architecture and T cell abundance in lymphoid organs (**Supplementary Figs. 4** and **5**). In contrast, rapamycin did not fully preserve splenic architecture or T cell counts in the p190 model (**Supplementary Figs. 4** and **5b**). PP242 in combination with

dasatinib significantly inhibited the proliferation and survival of human B-ALL cells *in vivo* while allowing hematopoietic expansion of endogenous mouse bone marrow (**Fig. 5c**,**d**,**g** and **Supplementary Fig. 6b**). In human hematopoietic colony-forming assays (**Fig. 6a**), rapamycin was myelosuppressive at much lower concentrations than PP242. The dual PI3K-mTOR inhibitor PI-103 had comparable effects to PP242 in these colony-forming assays (**Fig. 6a**). Considering that the GI_{50} of PI-103 in cancer cell lines was twofold to sevenfold greater than that of PP242, it was striking that PI-103 showed a much greater hematotoxicity at a dose (2 μM) that was twofold higher than the highest dose tested of PP242 (1 μM) (**Fig. 6a**). We also observed that p190 cell-transplanted mice treated with imatinib and a therapeutic dose of PI-103 (60 mg per kg body weight b.i.d.), but not imatinib plus a therapeutic dose of PP242 (60 mg per kg body weight once daily (q.d.)), had reduced cycling of endogenous bone marrow cells (**Fig. 4e**).

PP242 showed consistently weaker effects than rapamycin in assays of adaptive immune function. Rapamycin (1–10 nM) strongly suppressed *ex vivo* B and T cell proliferation (**Fig. 6b–d** and **Supplementary Fig. 7**). In contrast, PP242 had little effect at 1–10 nM, with increasing effects at 100 nM and 1 μM, the latter far exceeding its effective concentration for inhibiting growth in leukemia cell lines (**Fig. 1b**). The reduced antiproliferative potency of PP242 in primary lymphocytes compared to leukemia cells was not due to differences in its effects on TORC1/2 signaling, as the compound inhibited phosphorylation of Akt, 4E-BP1 and rS6 (**Supplementary Fig. 7c**) at concentrations similar to those found to be effective in p190 cells (**Fig. 2a**,**b**). PP242 also decreased the size of activated T cells, which we also observed in PP242-treated leukemia cells (**Supplementary Fig. 3**) and can be considered a surrogate readout for TORC1 inhibition (**Fig. 6d**). As observed in human hematopoietic colony assays, PI-103 suppressed normal B cell proliferation much more strongly than did PP242 when tested at a twofold higher concentration (**Fig. 6c**). Another pan–PI3K-TORC1/2 inhibitor, BEZ-235, suppressed T cell proliferation more strongly than did PP242 when tested at the same concentration (**Fig. 6d** and **Supplementary Fig. 7b**). Similarly to PP242, the TORC1/2 inhibitor Ku-0063794 had little effect on B cell proliferation at a concentration of 100 nM (**Fig. 6c**) and partially inhibited the response at 1 μM (data not shown).

To compare the effects of PP242 and rapamycin on adaptive immunity *in vivo*, we measured antibody responses to the $CD4^+$ T cell–dependent antigen nitrophenyl-ovalbumin (NP-OVA). We treated mice orally with PP242 (60 mg per kg body weight), a dose that achieved rapid leukemic clearance in other experiments (**Fig. 4** and **5**) or with rapamycin (7.5 mg per kg body weight) starting 1 day before immunization. Whereas rapamycin strongly lowered nitrophenyl-specific antibody titers, PP242 had little or no effect (**Fig. 6e**). These patterns were reflected in the percentage of B cells with a germinal center phenotype (**Fig. 6f**). Furthermore, rapamycin treatment lowered the percentages of total T and B cells in the spleen, whereas PP242 did not (**Fig. 6g**). In a separate experiment, we tested PI-103 at 10, 30 and 60 mg per kg body weight b.i.d. Although PI-103-treated mice developed nitrophenyl-specific antibody titers that were equivalent to those in vehicle- or PP242-treated mice (**Fig. 6e**), PI-103 reduced the fraction of B cells with a germinal center phenotype (**Fig. 6f**) and lowered the percentages of total splenic B and T cells (**Fig. 6g**). PI-103 also caused a dose-dependent displacement of marginal zone B cells (**Supplementary Fig. 8**), a surrogate readout for PI3K (p110δ) inhibition[43].

DISCUSSION

We show here that a selective, active-site mTOR kinase inhibitor has potent antileukemic effects *in vitro* and *in vivo*, while leaving lymphocyte function largely intact. Active-site inhibition of TORC1/2 addresses rapamycin-resistant TORC1 outputs and prevents activation of AKT resulting from feedback regulation (**Fig. 1a**). TORC1/2 inhibition caused selective apoptosis of leukemic cells and also synergized with clinically relevant TKIs in assays of both mouse and human leukemic expansion. A likely mechanism is that the PI3K-mTOR pathway is sustained by cytokines and serum factors even when BCR-ABL kinase activity is inhibited. These findings support the importance of TORC1/2 as a druggable target downstream of BCR-ABL in a disease in which resistance to TKIs develops rapidly. TORC1/2 inhibitors might be particularly effective when used with current induction regimens consisting of dasatinib with or without chemotherapy for treating Ph^+ B-ALL .

Whereas PP242 is toxic to leukemia cells, normal hematopoietic cells and mature lymphocytes survive in mice treated with therapeutic doses. Moreover, lymphocyte function shows an inverse pattern of drug sensitivity relative to leukemia cells, with rapamycin having more potent suppressive effects than PP242. The finding that pharmacological TORC1/2 inhibition is tolerated by the adaptive immune system was unexpected, considering that complete deletion of the gene encoding mTOR (*Mtor*) in mouse T cells has more severe effects on proliferation[44]. One possibility is that mTOR has a noncatalytic scaffolding function that is abolished by gene deletion or rapamycin treatment but not by the active-site kinase inhibitor. Another possibility is that PP242 does not provide sustained blockade of mTOR kinase activity through a dosing regimen that achieves therapeutic antileukemic effects; temporary inhibition of mTOR signaling outputs could be more detrimental to cancer cells, in which transient signaling interruption can commit the cell irreversibly to death through an effect termed 'oncogenic shock'[45]. At higher concentrations of PP242, lymphocyte proliferation was strongly suppressed *in vitro*. Of note, mice heterozygous for an allele of *Mtor* encoding a kinase-dead version of mTOR show normal lymphocyte proliferation[46], supporting the idea that partial or temporary TORC1/2 kinase inhibition is tolerated by normal lymphocytes.

A key question is whether selective TORC1/2 inhibitors provide advantages over pan–PI3K-TORC1/2 pathway inhibitors. PI3K has numerous roles in cell survival, differentiation, metabolism and migration, some of which are independent of AKT and mTOR[1,47]. Our data suggest that whereas TORC1/2 and pan–PI3K-TORC1/2 inhibitors both have antileukemic efficacy, the pan–PI3K-TORC1/2 inhibitors cause greater immune suppression. When we tested PI-103 at a twofold higher concentration than PP242, given the consistently twofold higher GI_{50} of PI-103 in cancer cell lines, we observed greater suppression of hematopoietic colony formation and B cell proliferation. *In vivo* treatment of mice with PI-103 at concentrations that had antileukemic effects also lowered the abundance of key lymphocyte subsets that were unaffected by treatment with PP242. A recent report also found that PI-103 lowers lymphocyte numbers *in vivo* and showed that PI-103 suppresses immune rejection of melanoma xenografts[48]. It remains to be seen whether pan–PI3K-TORC1/2 inhibitors will provide an acceptable therapeutic window in humans. Our data indicate that selective TORC1/2 inhibition is an attractive alternative approach that provides equivalent antileukemic efficacy as pan–PI3K-TORC1/2 inhibitors while maintaining PI3K activity.

Overall, these findings provide encouragement for further preclinical and clinical studies of selective active-site mTOR inhibitors in cancer. Given the efficacy of PP242 when combined with dasatinib in Ph^+ B-ALL xenografts, therapy that combines TORC1/2 kinase inhibitors with TKIs that target other oncogenic 'driving' mutations may improve treatment outcomes in other leukemias and in epithelial malignancies.

METHODS

Methods and any associated references are available in the online version of the paper at http://www.nature.com/nm/.

Note: Supplementary information is available on the Nature Medicine website.

ACKNOWLEDGMENTS

We thank K. Shokat, T. Wilson, and M. Kharas for support and helpful discussions and R. Nguyen for constructing BCR-ABL mutants. For access to the LSM710 Zeiss confocal microscope we thank E. Gratton's laboratory in the Department of Biomedical Engineering, University of California–Irvine. The SUP-B15 cells stably expressing firefly luciferase (SUP-B15^{ffLuc}) were a kind gift from M. Jensen (City of Hope). Technical assistance was provided through the Optical Biology Core facility of the Developmental Biology Center, a shared resource supported in part by the Cancer Center Support Grant (CA-62203) and the Center for Complex Biological Systems Support Grant (GM-076516) at the University of California–Irvine. The Lumina IVIS bioluminescent imager was supported by a grant to the University of California–Irvine from the California Institute of Regenerative Medicine. This work was supported by US National Institutes of Health training grant T32-CA009054 (to M.R.J.), National Institutes of Health Minority Access to Research Careers grant T34GM069337 (to M.A.C.), a Research Scholar Grant from the American Cancer Society (to D.A.F.), a Discovery Grant from the University of California Industry–University Cooperative Research Program (to D.A.F.), a sponsored research agreement from Intellikine, Inc. (to D.A.F.) and a Bridge award from the Chao Family Comprehensive Cancer Center. M.R.J. is an awardee of the Jackie Murphy and Carol Malouf Scholar Achievement Rewards for College Scientists.

AUTHOR CONTRIBUTIONS

M.R.J. designed and performed experiments, analyzed data and wrote the manuscript. J.J.L., L.S., J.C. and C.V. designed and performed experiments and analyzed data. M.A.C., R.J.L. and S.M. performed experiments and analyzed data. M.B.L., S.T.O. and M.K. provided clinical samples, analyzed data and edited the manuscript. M.B.M. and P.R. provided materials and supervised groups performing chemical synthesis and formulation. Y.L. and C.R. designed and supervised experiments and edited the manuscript. D.A.F. designed and supervised experiments and wrote the manuscript.

COMPETING INTERESTS STATEMENT

The authors declare competing financial interests: details accompany the full-text HTML version of the paper at http://www.nature.com/naturemedicine/.

Published online at http://www.nature.com/naturemedicine/.
Reprints and permissions information is available online at http://npg.nature.com/reprintsandpermissions/.

1. Engelman, J.A., Luo, J. & Cantley, L.C. The evolution of phosphatidylinositol 3-kinases as regulators of growth and metabolism. *Nat. Rev. Genet.* **7**, 606–619 (2006).
2. Manning, B.D. & Cantley, L.C. AKT/PKB signaling: navigating downstream. *Cell* **129**, 1261–1274 (2007).
3. Samuels, Y. & Ericson, K. Oncogenic PI3K and its role in cancer. *Curr. Opin. Oncol.* **18**, 77–82 (2006).
4. Martelli, A.M. *et al.* Involvement of the phosphoinositide 3-kinase/Akt signaling pathway in the resistance to therapeutic treatments of human leukemias. *Histol. Histopathol.* **20**, 239–252 (2005).
5. Wee, S. *et al.* PI3K pathway activation mediates resistance to MEK inhibitors in KRAS mutant cancers. *Cancer Res.* **69**, 4286–4293 (2009).
6. Yap, T.A. *et al.* Targeting the PI3K-AKT-mTOR pathway: progress, pitfalls and promises. *Curr. Opin. Pharmacol.* **8**, 393–412 (2008).
7. Abraham, R.T. Regulation of the mTOR signaling pathway: from laboratory bench to bedside and back again. *F1000 Biology Reports* **1**, 8 (2009).
8. Guertin, D.A. & Sabatini, D.M. Defining the role of mTOR in cancer. *Cancer Cell* **12**, 9–22 (2007).
9. Abraham, R.T. & Eng, C.H. Mammalian target of rapamycin as a therapeutic target in oncology. *Expert Opin. Ther. Targets* **12**, 209–222 (2008).
10. Guertin, D.A. & Sabatini, D.M. The pharmacology of mTOR inhibition. *Sci. Signal.* **2**, pe24 (2009).
11. Janes, M.R. & Fruman, D.A. Immune regulation by rapamycin: moving beyond T cells. *Sci. Signal.* **2**, pe25 (2009).
12. Thomson, A.W., Turnquist, H.R. & Raimondi, G. Immunoregulatory functions of mTOR inhibition. *Nat. Rev. Immunol.* **9**, 324–337 (2009).
13. Choo, A.Y., Yoon, S.O., Kim, S.G., Roux, P.P. & Blenis, J. Rapamycin differentially inhibits S6Ks and 4E-BP1 to mediate cell-type-specific repression of mRNA translation. *Proc. Natl. Acad. Sci. USA* **105**, 17414–17419 (2008).
14. Feldman, M.E. *et al.* Active-Site Inhibitors of mTOR target rapamycin-resistant outputs of mTORC1 and mTORC2. *PLoS Biol.* **7**, e38 (2009).
15. García-Martínez, J.M. *et al.* Ku-0063794 is a specific inhibitor of the mammalian target of rapamycin (mTOR). *Biochem. J.* **421**, 29–42 (2009).
16. Thoreen, C.C. *et al.* An ATP-competitive mammalian target of rapamycin inhibitor reveals rapamycin-resistant functions of mTORC1. *J. Biol. Chem.* **284**, 8023–8032 (2009).
17. Yu, K. *et al.* Biochemical, cellular and *in vivo* activity of novel ATP-competitive and selective inhibitors of the mammalian target of rapamycin. *Cancer Res.* **69**, 6232–6240 (2009).
18. Chiarini, F. *et al.* Dual inhibition of class IA phosphatidylinositol 3-kinase and mammalian target of rapamycin as a new therapeutic option for T-cell acute lymphoblastic leukemia. *Cancer Res.* **69**, 3520–3528 (2009).
19. Kharas, M.G. *et al.* Ablation of PI3K blocks BCR-ABL leukemogenesis in mice, and a dual PI3K/mTOR inhibitor prevents expansion of human BCR-ABL$^+$ leukemia cells. *J. Clin. Invest.* **118**, 3038–3050 (2008).
20. Kojima, K., *et al.* The dual PI3 kinase/mTOR inhibitor PI-103 prevents p53 induction by Mdm2 inhibition but enhances p53-mediated mitochondrial apoptosis in p53 wild-type AML. *Leukemia* **22**, 1728–1736 (2008).
21. Park, S. *et al.* PI-103, a dual inhibitor of class IA phosphatidylinositide 3-kinase and mTOR, has antileukemic activity in AML. *Leukemia* **22**, 1698–1706 (2008).
22. Burgess, M.R. & Sawyers, C.L. Treating imatinib-resistant leukemia: the next generation targeted therapies. *ScientificWorldJournal* **6**, 918–930 (2006).
23. Druker, B.J. Translation of the Philadelphia chromosome into therapy for CML. *Blood* **112**, 4808–4817 (2008).
24. Li, S., Ilaria, R.L. Jr., Million, R.P., Daley, G.Q. & Van Etten, R.A. The P190, P210 and P230 forms of the BCR/ABL oncogene induce a similar chronic myeloid leukemia-like syndrome in mice but have different lymphoid leukemogenic activity. *J. Exp. Med.* **189**, 1399–1412 (1999).
25. Raynaud, F.I. *et al.* Pharmacologic characterization of a potent inhibitor of class I phosphatidylinositide 3-kinases. *Cancer Res.* **67**, 5840–5850 (2007).
26. Maira, S.M. *et al.* Identification and characterization of NVP-BEZ235, a new orally available dual phosphatidylinositol 3-kinase/mammalian target of rapamycin inhibitor with potent *in vivo* antitumor activity. *Mol. Cancer Ther.* **7**, 1851–1863 (2008).
27. Gruber, F., Mustjoki, S. & Porkka, K. Impact of tyrosine kinase inhibitors on patient outcomes in Philadelphia chromosome–positive acute lymphoblastic leukaemia. *Br. J. Haematol.* **145**, 581–597 (2009).
28. Talpaz, M. *et al.* Dasatinib in imatinib-resistant Philadelphia chromosome–positive leukemias. *N. Engl. J. Med.* **354**, 2531–2541 (2006).
29. Hu, Y. *et al.* Targeting multiple kinase pathways in leukemic progenitors and stem cells is essential for improved treatment of Ph$^+$ leukemia in mice. *Proc. Natl. Acad. Sci. USA* **103**, 16870–16875 (2006).
30. McCubrey, J.A. *et al.* Targeting survival cascades induced by activation of Ras/Raf/MEK/ERK, PI3K/PTEN/Akt/mTOR and Jak/STAT pathways for effective leukemia therapy. *Leukemia* **22**, 708–722 (2008).
31. Foa, R. *et al.* Line treatment of adult Ph$^+$ acute lymphoblastic leukemia (ALL) patients. Final results of the GIMEMA LAL1205 study. *Blood* **112**, abstract 305 (2008).
32. Prabhu, S. *et al.* A novel mechanism for Bcr-Abl action: Bcr-Abl-mediated induction of the eIF4F translation initiation complex and mRNA translation. *Oncogene* **26**, 1188–1200 (2007).
33. Zhang, M. *et al.* Inhibition of polysome assembly enhances imatinib activity against chronic myelogenous leukemia and overcomes imatinib resistance. *Mol. Cell. Biol.* **28**, 6496–6509 (2008).
34. Hedrick, S.M. The cunning little vixen: Foxo and the cycle of life and death. *Nat. Immunol.* **10**, 1057–1063 (2009).
35. Huang, H. & Tindall, D.J. Dynamic FoxO transcription factors. *J. Cell Sci.* **120**, 2479–2487 (2007).
36. Copp, J., Manning, G. & Hunter, T. TORC-specific phosphorylation of mammalian target of rapamycin (mTOR): phospho-Ser2481 is a marker for intact mTOR signaling complex 2. *Cancer Res.* **69**, 1821–1827 (2009).
37. García-Martínez, J.M. & Alessi, D.R. mTOR complex 2 (mTORC2) controls hydrophobic motif phosphorylation and activation of serum- and glucocorticoid-induced protein kinase 1 (SGK1). *Biochem. J.* **416**, 375–385 (2008).
38. Kennedy, J.A. & Barabe, F. Investigating human leukemogenesis: from cell lines to *in vivo* models of human leukemia. *Leukemia* **22**, 2029–2040 (2008).
39. Sarbassov, D.D. *et al.* Prolonged rapamycin treatment inhibits mTORC2 assembly and Akt/PKB. *Mol. Cell* **22**, 159–168 (2006).
40. Mohi, M.G. *et al.* Combination of rapamycin and protein tyrosine kinase (PTK) inhibitors for the treatment of leukemias caused by oncogenic PTKs. *Proc. Natl. Acad. Sci. USA* **101**, 3130–3135 (2004).
41. Luo, F.R. *et al.* Dasatinib (BMS-354825) pharmacokinetics and pharmacodynamic biomarkers in animal models predict optimal clinical exposure. *Clin. Cancer Res.* **12**, 7180–7186 (2006).
42. Sankhala, K. *et al.* The emerging safety profile of mTOR inhibitors, a novel class of anticancer agents. *Target. Oncol.* **4**, 135–142 (2009).
43. Durand, C.A. *et al.* Phosphoinositide 3-kinase p110δ regulates natural antibody production, marginal zone and B-1 B cell function, and autoantibody responses. *J. Immunol.* **183**, 5673–5684 (2009).
44. Delgoffe, G.M. *et al.* The mTOR kinase differentially regulates effector and regulatory T cell lineage commitment. *Immunity* **30**, 832–844 (2009).
45. Sharma, S.V., Fischbach, M.A., Haber, D.A. & Settleman, J. 'Oncogenic shock': explaining oncogene addiction through differential signal attenuation. *Clin. Cancer Res.* **12**, 4392s–4395s (2006).
46. Shor, B., Cavender, D. & Harris, C. A kinase-dead knock-in mutation in mTOR leads to early embryonic lethality and is dispensable for the immune system in heterozygous mice. *BMC Immunol.* **10**, 28 (2009).
47. Fruman, D.A. & Bismuth, G. Fine tuning the immune response with PI3K. *Immunol. Rev.* **228**, 253–272 (2009).
48. Lopez-Fauqued, M., *et al.* The dual PI3K/mTOR inhibitor (PI-103) promotes immunosupression, *in vivo* tumor growth and increases survival of sorafenib treated melanoma cells. *Int. J. Cancer* published online, doi:10.1002/ijc.24926 (6 October 2009).

ONLINE METHODS

Chemical synthesis and inhibitors. We synthesized PP242 as described previously[49]. We obtained imatinib, dasatinib and rapamycin from LC Laboratories. We obtained LY294002 and PD98059 from Sigma-Aldrich. Some compounds were synthesized as described in patents (BEZ-235: patent WO 2006122806; IC87114: patent WO 2001081346; PI-103: patent WO 2001083456, TG101348, patent WO 2007053452; Ku-0063794, patent WO 2007060404).

Cell culture and viruses. We obtained SUP-B15 human Ph^+ B-ALL cells, K562 cells and solid tumor cell lines (SKOV3, PC-3, 786-O, U87) from the American Type Culture Collection. The SUP-B15 cells stably expressing firefly luciferase ($SUP\text{-}B15^{ffLuc}$) were a gift from M. Jensen (City of Hope). We introduced p190 BCR-ABL (or mutated versions) and a surface marker for FACS detection (human CD4) into hematopoietic cells by infection with retroviruses, which we obtained by transient transfection of 293T cells with various pMSCV vectors as we have previously reported[19]. We infected mouse hematopoietic cells using standard procedures as detailed in the **Supplementary Methods.**

***In vitro* cell viability studies, cap pull-down assay and protein expression analysis.** We performed cell viability assays, retroviral transduction, cap pull-down, western blot, flow cytometry assays and confocal fluorescence microscopy following standard procedures as detailed in the **Supplementary Methods**.

Mice. We kept all mice in specific pathogen–free animal facilities at the University of California, Irvine; all mouse procedures were performed in accordance with the guidelines of the Institutional Animal Care and Use Committee of University of California–Irvine. We used 8-week-old female BALB/cJ (Jackson Laboratory) mice as recipients of mouse p190 BCR-ABL–transformed bone marrow as has been previously described[19]. We used 6- to 12-week-old male and female NSG (JAX mouse stock name NOD.Cg-*Prkdc*^{scid} *Il2rg*^{tm1Wjl}*/SzJ*; Jackson Laboratory) as recipients for human leukemic transplants[38]. We used 8-week-old female C57BL/6J (Jackson Laboratory) mice for immunization experiments and 6–8-week-old BALB/cJ (Jackson Laboratory) mice for *ex vivo* lymphocyte cultures.

Primary leukemia samples. Cryopreserved peripheral blood samples, provided by one of the authors (M.B.L.), were obtained from subjects during treatment at Loma Linda Medical Center. Heparanized peripheral blood was collected during the course of routine clinical care or as part of a Loma Linda Medical Center Institutional Review Board–approved specimen bank protocol. The use of human samples for this study was approved by the University of California Irvine Institutional Review Board, with the stipulation that the samples lacked personal identifiers and that the donors were either deceased or had initially signed a specimen banking consent. We obtained cryopreserved bone marrow from the University of Texas M.D. Anderson Cancer Center with the approval of its Institutional Review Board. All bone marrow samples were collected during routine diagnostic procedures after informed consent was obtained in accordance with the regulations of the University of Texas M.D. Anderson Cancer Center and the Declaration of Helsinki. Brief clinical histories and pathological characteristics of human samples are further detailed in the **Supplementary Methods** and in **Supplementary Table 4**. Procedures for the isolation, purification and culturing of leukemic samples have been previously described[19].

Primary human bone marrow cultures. We used a contract service (Stem Cell Technologies) to compare the effects of inhibitors on human bone marrow colony formation. Details are provided in the **Supplementary Methods.**

Leukemia transplantation procedures. Transplantation, engraftment procedures, bioluminescent imaging procedures and flow cytometric evaluation of disease endpoints are detailed in the **Supplementary Methods**.

***In vivo* drug formulation and treatments.** Details of the formulation of all compounds are provided in the **Supplementary Methods**. For BALB/cJ recipients engrafted with p190 cells, we treated mice with dosing schedules as indicated in the figure legend (**Fig. 4**). For NSG recipients engrafted with $SUP\text{-}B15^{ffLuc}$ cells, we treated mice with daily doses of vehicle, dasatinib (2.5 mg per kg body weight, p.o.) alone or in combination with rapamycin (7.5 mg per kg body weight, i.p.) or PP242 (60 mg per kg body weight, p.o.) throughout the full treatment duration. All recipients received both p.o. and i.p. doses of vehicle or equivalent to control for morbidity associated with treatment procedures and mouse handling. For NSG recipients engrafted with primary human bone marrow samples, we treated mice with daily doses (5 consecutive d per week, allowing mice to have a 2-d rest without any treatments or handling) of vehicle, dasatinib (5 mg per kg body weight, p.o.) alone or in combination with PP242 (60 mg per kg body weight, p.o.). For C57BL/6J mice used for NP-OVA immunizations, we treated the mice with dosing schedules as indicated in the figure legends (**Fig 6** and **Supplementary Fig. 8**).

Immunizations and measurement of nitrophenyl-specific immunoglobulin. We immunized mice with NP(15)-OVA (Biosearch Technologies) in Imject Alum (Pierce) at a concentration of 0.5 mg ml^{-1} (50 μg per mouse) by i.p. injection. We killed the mice 8 d after immunization for immune assessment. We detected serum immunoglobulin by ELISA using standard procedures that are further detailed in the **Supplementary Methods**.

Statistical analyses. To validate the significance of the observed differences, we analyzed random continuous variables using two-sided *t* tests, one-way ANOVA, repeated measures ANOVA and two-way ANOVA. We used Tukey-Kramer *post-hoc* analysis for all comparisons. We compared differences in survival using the log-rank test. We calculated homogeneity of variances by Bartlett's test. We used two-tailed Pearson's correlation to find correlation between continuous variables. We used GraphPad Prism (4.0c) software for all statistical analyses.

49. Apsel, B. *et al.* Targeted polypharmacology: discovery of dual inhibitors of tyrosine and phosphoinositide kinases. *Nat. Chem. Biol.* **4**, 691–699 (2008).